Vietnam Journal of Catalysis and Adsorption
Tạp chí xúc tác và hấp phụ Việt Nam

http://chemeng.hust.edu.vn/jca/

Dyes adsorption properties of odered mesoporous carbon material using mcf silica as hard template

Hoa T.H.Nguyen[1*], Linh T.N.Linh[1], Quy M.Bui[1] and Phuong T.Dang[2]

[1] *Faculty of Chemistry, TNU - University of Sciences, Thai Nguyen, VIETNAM*
[2] *Institute of Chemistry, Vietnam Academy of Science and Technology (VAST) - 18 Hoang Quoc Viet, Cau Giay, Hanoi, VIETNAM*
**Email: hoanth@tnus.edu.vn*

ARTICLE INFO

Received: 12/11/2021
Accepted: 20/3/2022
Published: 25/3/2022

Keywords:

Ordered mesoporous carbons materials, MCF template, Methylene blue, Red phenol, Direct blue 71, dye adsorption

ABSTRACT

Ordered mesoporous carbon materials using MCF silica as hard template (OMC(MCF)) were synthesized. The synthesized OMC(MCF) materials were characterized by different techniques such as XRD, TEM, BET. The results revealed that the surface area, pore volume and pore size of OMC (MCF) were of 1,073 m^2 /g, 1.35 cm^3 /g and 5.7 nm, respectively. The dye adsorption experiments were carried out through a batch test to evaluate synthesized OMC(MCF) materials. Methylene blue (MB- cationic dye), phenol red (PR - anionic dye) and direct blue 71 dyes (DB71- anionic dye) were chosen as adsorbates. Negatively charged surfaces OMC(MCF) materials have better adsorption capacity for positively charged methylene blue than that of negatively charged direct blue 71 and phenol red. OMC(MCF) materials could be used as a potential adsorbent for the removal of positive charged organic dyes.

Introduction

Porous carbon materials [1, 2, 3] are of scientific and technological importance due to their unique properties (high surface area, pore size and large porosity, high adsorption capacity of bulky large molecules, high chemical and thermal stability, etc.). Therefore, porous carbon is widely used in many applications such as gas separation [4], adsorbents [5-8], gas storage [9], catalysts [10, 11], electrochemical energy storage [12]. Most porous carbons are usually obtained via carbonization carbon precursor. Porous carbons are synthesized by hard – temlating method using nanostructured silica as template to impregnate with an appropriate carbon source, followed by carbonization of the composite, and subsequent removal of the template [13].

Using solid adsorbent to treat polluted organic matter in the water environment is considered a "green" method because of the advantages such as: fast, thorough treatment process, without adding chemicals to the environment, easy to fabricate, reusable adsorbent material and no secondary pollution. Methylene blue (MB) and direct blue 71 dyes (DB71) are two imporant dyes which are widely used in textile industry. Phenol red (PR) is a pH indicator frequently used in cell biology laboratories. Some general physicochemical properties of MB, PR and DB71 are presented in Table 1.

https://doi.org/10.51316/jca.2022.047

Porous carbon materials can be synthesized by the hard method. Siliceous mesostructured cellular foams (MCF) as the surfactant because it has well-defined, large pore sizes**,** a high specific surface area and it easy removed by HF.

In this paper, we report the synthesis of OMC(MCF) by hard template method using MCF as surfactant. With our knowledge, this is first study about synthesis, characterization and MB, PR and DB71 adsorption properties of OMC(MCF).

Table 1: The main properties of the selected adsorbates

Molecule/ Formula	Structure
Methylene blue / $C_{16}H_{18}N_3SCl$	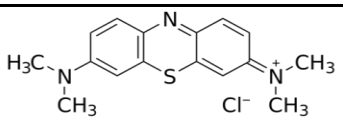
Phenol red / $C_{19}H_{14}O_5S$	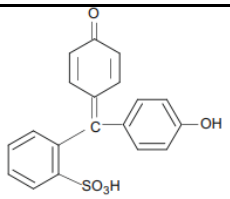
Direct blue 71 / $C_{40}H_{23}N_7Na_4O_{13}S_4$	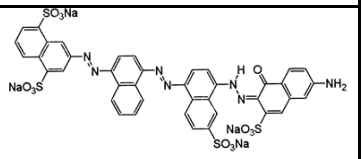

Experimental

Synthesis of OMC(MCF)

MCF silica were synthesized with a triblock copolymer, $EO_{20}PO_{70}EO_{20}$ (Pluronic P123, Aldrich), as the surfactant, and liquid glass as the silica source. Namely, Dissolve P123 in water until the solution is clear at room temperature. Add to a solution HCl 4M, NH_4F. Add to TMB, mechanical stirring with speed 1000 rpm, temperature 40°C for 1 hour. Add to TEOS, mechanical stirring with speed 1000 rpm, temperature 40°C for 2 hours. The mixture was stirred at temperature 40°C for 24 hours. The mixture was crystallized in a teflon bottle at 100°C, for 24 hours.The sample was washed to pH = 7. The sample was calcined for 2 hours at 300 °C, then 4 hours at 550 °C.

OMC(MCF) was synthesized with MCF as the template, sucrose as carbon sources. Namely, 1g of sucrose and 1g MCF were mixed well. Added to a solution H_2SO_4 (0.14g of H_2SO_4 in 5g of H_2O), stirred for 30 minutes. The mixture was placed in a drying oven for 6 hours at 100°C, and then the oven temperature was increased to 160°C for 6 hours. This step was repeated one more time. The carbonization was calcined at 800°C under nitrogen flow. The silica – carbon material was immerged in HF 40% solution and then washed with H_2O before being washed with a mixture of 50 vol% ethanol + 50 vol% H_2O. The obtained OMC (MCF) material was dried at 100°C for 3 hours.

Characterization

The powder X-ray diffraction (XRD) analysis was performed using on a Shimadzu XRD-6100 analyzer with Cu K_α radiation (λ = 1.5417Å). The morphologies and microstructures were investigated by Transmission electron microscopy (TEM, JEOL1010 instrument operating at 80 kV with a magnification of 25,000 – 100,000). The surface area of samples was determined on Quantachrome Instruments version 3.0 at 77K and using nitrogen as an adsorbent.

Adsorption experiments

Adsorption experiments were conducted by varying the initial concentration (100 – 300 ppm), the adsorbent (The methylene blue (MB - $C_{16}H_{18}N_3SCl$), phenol red (PR - $C_{19}H_{14}O_5S$) and direct blue 71 (DB71 - $C_{40}H_{23}N_7Na_4O_{13}S_4$)). They were carried out in liquid phase at 25°C under stirring condition.
Adsorption capacity (Q_t) of MB is denied as follows:

$$Q_t = \frac{(C_0 - C_t)V}{m} \quad (1)$$

Where Q_t is adsorption capacity of MB or PR or DB71; V is solution volume (V = 0.1L); m is masses of OMC (MCF); C_0 and C_t (ppm) are initial and time t MB or PR or DB71 concentration.

Equilibrium concentration of MB, PR and DB71 were determined by a UV-VIS spectrophotometer (UV - vis - 1700) at a λ_{max} of 664 nm, 435 nm and 587 nm, respectively.

Adsorption isotherms

Langmuir and Freundlich isotherms models, were often used to analyze the experimental data [2]. The Langmuir equation is expressed as follows:

$$\frac{C_e}{Q_e} = \frac{1}{Q_m.K_L} + \left(\frac{1}{Q_m}\right).C_e \quad (2)$$

The Freundlich equation is expressed as follows:

https://doi.org/10.51316/jca.2022.047

$$\log Q_e = \log K_F + \left(\frac{1}{n}\right).\log C_e \quad (3)$$

Where Q_m and K_L in the Langmuir equation represent the maximum adsorption capacity of adsorbents (mg/g) and Langmuir adsorption constant related to the free energy of adsorption, respectively. K_F and n are Freundlich constants related to adsorption capacity and adsorption intensity, respectively.

Results and discussion

Characterization

XRD patterns and TEM images of MCF and OMC(MCF) samples are shown in Figure 1. From XRD patterns of MCF and OMC(MCF) (Figure 1a) showed that OMC(MCF) had the same structure with MCF. In Figure 1b, MCF material has a porous size of about 20 nm. In Figure 1c, the ordered structures OMC(MCF) samples with hexagonal symmetry and uniform pore dimension were clearly observed.

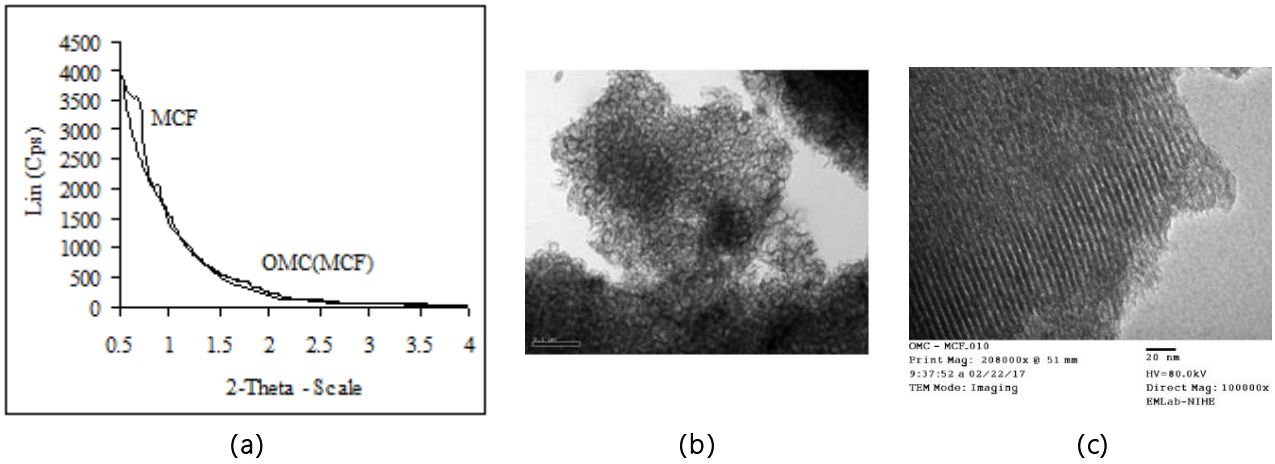

(a) (b) (c)

Figure 1: XRD patterns of MCF and OMC(MCF) (a); TEM images of MCF (b); TEM images of OMC(MCF) (c)

N_2 adsorption–desorption isotherms and pore-size distribution of MCF and OMC(MCF) are presented in Figure 2. The N_2 adsorption–desorption isotherms of MCF, OMC(MCF) showed the isotherm curves of type IV with the hysteresis loop, characteristic for capillary condensation which is typical for mesoporous material.

The pore-size distribution of MCF and OMC(MCF) showed OMC had average pore sizes of 23,5 nm; 13,9 nm and pore volume of 2,3 cm^3/g. OMC(MCF) had average pore size of 5.7 nm and pore volume of 1.35 cm^3/g. OMC(MCF) had a surface area of 1073 m^2/g higher than OMC had that of 520 m^2/g.

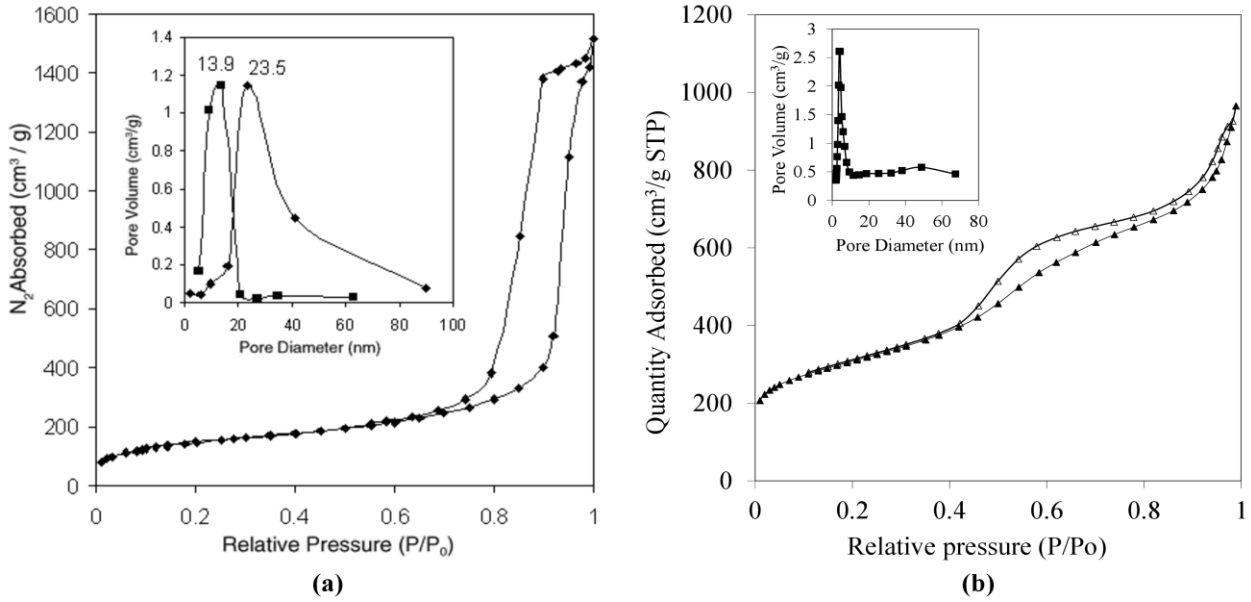

Figure 2: N_2 adsorption–desorption isotherms and pore-size distribution of MCF (a) and OMC(MCF) (b)

https://doi.org/10.51316/jca.2022.047

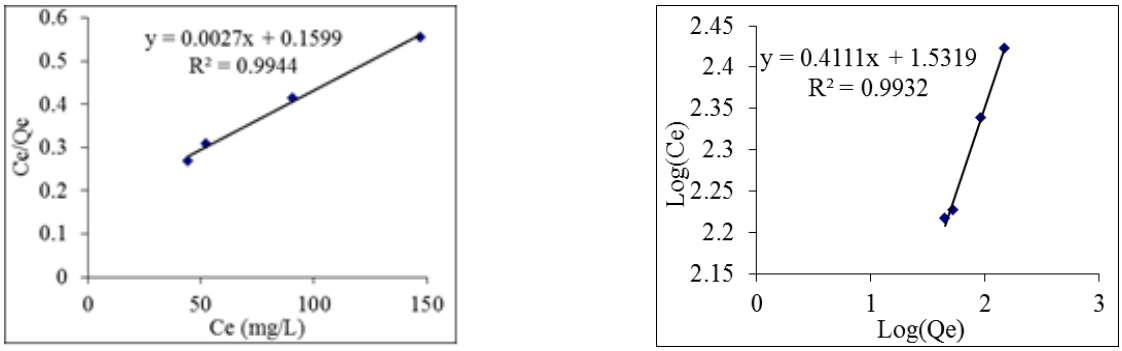

(a) (b)

Figure 3: Experimental DB71 adsorption data fitted to different isotherm models: (a) Langmuir and (b) Freundlich of OMC(MCF)

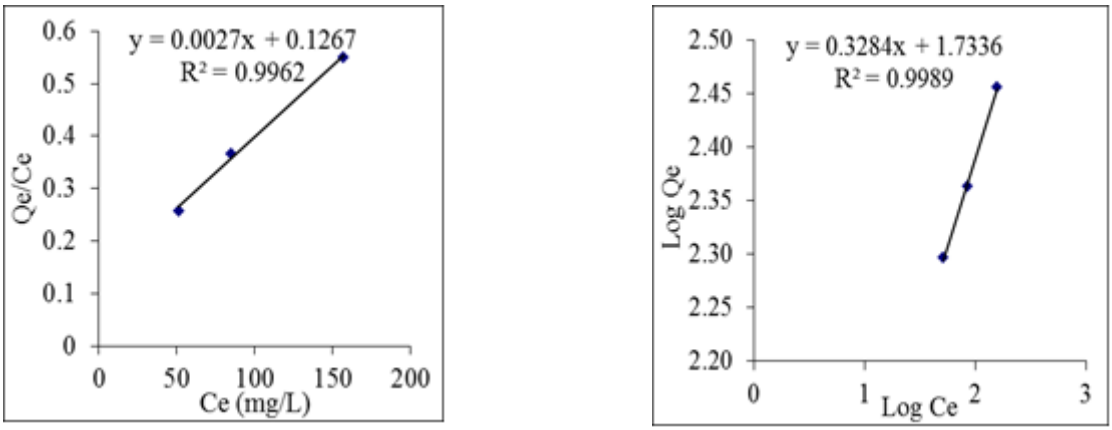

(a) (b)

Figure 4: Experimental PR adsorption data fitted to different isotherm models: (a) Langmuir and (b) Freundlich of OMC(MCF)

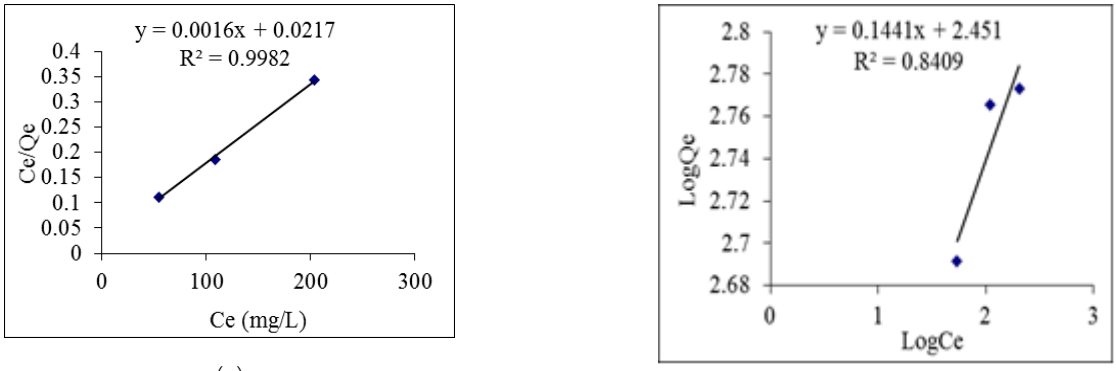

(a) (b)

Figure 5: Experimental MB adsorption data fitted to different isotherm models: (a) Langmuir and (b) Freundlich of OMC(MCF)

https://doi.org/10.51316/jca.2022.047

Adsorption Isotherms

MB, PR and DB71 were selected as adsorbates in this study. PR and DB71 are all anionic dyes of different molecular sizes. PR has a relatively smaller molecular size than that of DB71. PR and MB have similar molecular weights. PR is anionic dye, MB is cationic dye.

Table 2: Langmuir and Freundlich adsorption isotherm parameters of OMC(MCF) for MB, PR and DB71

Langmuir and Freundlich adsorption isotherm parameters of OMC(MCF) for DB71			
Langmuir isotherm		Freundlich isotherm	
Q_m (mg.g^{-1})	370	n	29.0
K_L (L.mg^{-1})	0.02	K_F (mg.g^{-1})	34.03
R^2	0.9944	R^2	0.9932
Langmuir and Freundlich adsorption isotherm parameters of OMC(MCF) for PR			
Q_m (mg.g^{-1})	370	n	3.0
K_L (L.mg^{-1})	0.02	K_F (mg.g^{-1})	54.15
R^2	0.9962	R^2	0.9932
Langmuir and Freundlich adsorption isotherm parameters of OMC(MCF) for MB			
Q_m (mg.g^{-1})	625	n	6.9
K_L (L.mg^{-1})	0.07	K_F (mg.g^{-1})	1.76
R^2	0.9982	R^2	0.8404

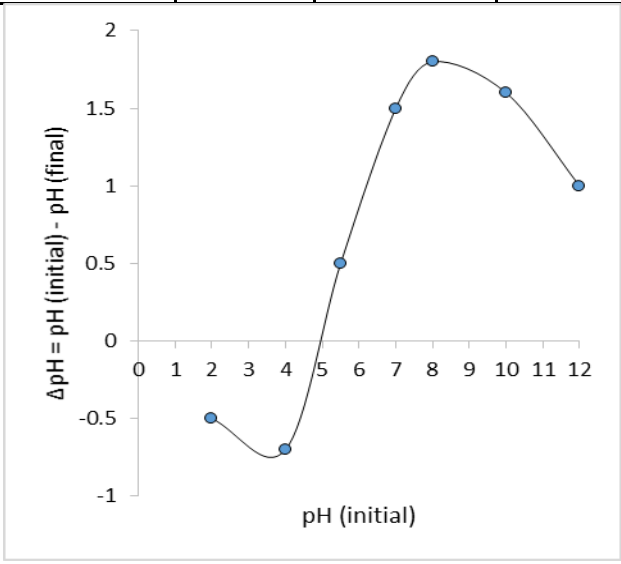

Figure 6: Determination of OMC(MCF) isoelectric point

MB, PR and DB71 adsorption capacities of OMC(MCF) are given in Figure 3, 4, 5 and Table 2, Q_m adsorption capacities of OMC(MCF) for MB, PR and DB71 are 625 mg/g, 370 mg/g and 370 mg/g, respectively.

PR and DB71 are anionic dyes. Q_m adsorption capacities of OMC(MCF) for PR (370 mg/g) were as high as for DB71 (370 mg/g). This can be explained that the greater the surface area of a material, the greater the adsorption capacity. OMC(MCF) had high surface area of 1073 m^2/g. Moreover, the average pore size of OMC (MCF) (5.7 nm) is greater than that of PR and DB71 (3.0 nm) [14]. Therefore, PR or DB71 molecules can be easily diffuse into the pore of OMC(MCF).

PR and MB have similar molecular weights. Q_m adsorption capacities of OMC(MCF) for MB (625 mg/g) were higher than for PR (370 mg/g). The force of electrostatic interaction depends on the pH of the environment, the pH value specifies the charge of the material and adsorbent. In water at neutral pH, OMC(MCF) with zero charged point pH_o = 5.0 (Figure 6). So, PR are negatively charged, MB is positively charged. In addition, MB and PR are adsorbed on OMC(MCF) by mainly electrostatic force. This is process of multi-layered physical adsorption. That is why the adsorption capacity OMC(MCF) for MB is higher than PR.

As observed in Figure 3, 4, 5 and Table 2, the value of R^2= 0.9944, 0.9962 and 0.9982 in the Langmuir model, R^2= 0.9932, 0.9932 and 0.8404 in the Freundlich model for adsorption of DB71, PR and MB, respectively. These results were indicating that the Langmuir model fits much better than the Freundlich model for three adsorbates.

Conclusion

Ordered mesoporous carbons OMC(MCF) were successful synthesized by using hard template methods using MCF silica as template. From XRD, TEM and N_2 adsorption–desorption (BET) results, it revealed that the obtained OMC(MCF) had high surface area (1073 m^2/g), large pore volume and pore size (5.7 nm). MB, PR and DB71 are adsorbed on OMC(MCF) by electrostatic forces. Thus, negatively charged surfaces OMC(MCF) have better adsorption capacity for positive charged methylene blue (625 mg/g) than that of negatively charged red phenol (370 mg/g) direct blue 71 (370 mg/g).

https://doi.org/10.51316/jca.2022.047

References

1. S. Jun, S.H. Joo, R. Ryoo, M. Kruk, M. Jaroniec, Z. Liu, T. Ohsuna, O. Terasaki, J. Am. Chem. Soc. 122 (2000) 10712-10713. https://doi.org/10.1021/ja002261e
2. D. Barrera, M. Dávila, V. Cornette, J.C.A de Oliveira, R.H. López, K. Sapag, Micropor. Mesopor. Mater. 180 (2013) 71–78. https://doi.org/10.1016/j.micromeso.2013.06.028
3. M. Enterria, F. Suárez-García, A. Martínez-Alonso, J.M.D. Tascon, Micropor. Mesopor. Mater. 151 (2012) 390-396. https://doi.org/10.1016/j.micromeso.2011.10.004
4. N.F Nejad, E. Shams, M.K. Amini, J.C. Bennett, Micropor. Mesopor. Mater. 168 (2013) 239- 246. https://doi.org/10.1016/j.micromeso.2012.10.012
5. Y. Li, B. Yuan, J. Fu, S. Deng, X. Lu, J. Colloid Interface Sci. 408 (2013) 181–190. https://doi.org/10.1016/j.jcis.2013.07.037
6. J. Chen, F. Cao, S. Chen, M. Ni, X. Gao, K. Cen, Appl. Surf. Sci. 317 (2014) 26–34. https://doi.org/10.1016/j.apsusc.2014.08.067
7. Z. Ezzeddine, I. Batonneau-Gener, Y. Pouilloux, H. Hamad, J. Mol. Liq. 223 (2016) 763–770. https://doi.org/10.1016/j.molliq.2016.09.003
8. W. Libbrecht, A. Verberckmoes, J.W. Thybaut, P. V.D. Voort, J.D. Clercq, Carbon 116 (2017) 528-546. https://doi.org/10.1016/j.carbon.2017.02.016
9. C.C. Huang, Y.H. Li, Y.W. Wang, C.H. Chen, Int. J. Hydrogen Energy 38 (2013) 3994-4002. https://doi.org/10.1016/j.ijhydene.2013.01.081
10. C.Y. Ahn, J.Y. Cheon, S.H. Joob, J. Kim, J. Power Sources, 222 (2013) 477 – 482. https://doi.org/10.1016/j.jpowsour.2012.09.012
11. S. Liu, C. Lai, B. Li, C. Zhang, M. Zhang, D. Huang, L. Qin, H. Yi, X. Liu, F. Huang, X. Zhou, L. Chen, Chem. Eng. J. 384 (2020) 123304. https://doi.org/10.1016/j.cej.2019.123304
12. R. Fu, Z. Li, Y. Liang, L.I. Feng, X.U Fei, D. Wu, New Carbon Materials, 26 (2011) 171-179. https://doi.org/10.1016/S1872-5805(11)60074-7
13. R. Ryoo, S. H. Joo, M. Kruk, M. Jaroniec, Adv. Mater, 13 (2001) 677 - 681. https://doi.org/10.1002/1521-4095(200105)13:9<677::AID-ADMA677>3.0.CO;2-C
14. M. Hata, Y. Amano, M. Machida, F. Imazeki. Journal of Environmental Chemistry 25 2 (2015) 79 - 86. https://doi.org/10.5985/jec.25.79